



Evolution of pore-size distribution of intact loess and remolded loess due to consolidation

Jia-Ding Wang^{1,2} · Ping Li^{1,2} · Yan Ma¹ · Sai K. Vanapalli³

Received: 27 March 2018 / Accepted: 6 September 2018 / Published online: 12 September 2018
© Springer-Verlag GmbH Germany, part of Springer Nature 2018

Abstract

Purpose It is widely acknowledged that the mechanical behavior of a soil is significantly influenced by the soil microstructure; and the microstructure can evolve as a result of any mechanical, hydraulic, chemical or thermal change taken place on soil sample. The present study aimed to investigate the microstructures of intact loess and remolded loess and to explore the evolution of the microstructure and PSD (pore-size distribution) due to consolidation for both intact and remolded loess.

Materials and methods A loess from the Loess Plateau of China was used as test material. A series of intact loess specimens were consolidated to various vertical pressures in oedometer cells. The same loess was remolded at the optimum water content state to various compaction degrees using static compaction method. It is equivalent to consolidate the remolded loess with the least compaction degree under various stress levels. The microstructures of intact loess specimens after consolidation tests and remolded loess specimens are characterized using the SEM (scanning electron microscope) and MIP (mercury intrusion porosimetry) techniques. The micrographs and PSDs under various consolidation pressures (or compaction energies) were compared to investigate the evolution of the microstructure and PSD induced by mechanical loading for each kind of soil.

Results and discussion The microstructure of intact loess is more homogeneous and is less dependent on consolidation stress than remolded loess. In both soils, the pores with entrance diameter smaller than 6 μm are almost not influenced by consolidation. In intact loess, inter-aggregate pores with entrance diameter greater than 6 μm are compressed randomly due to loading. However, in remolded loess, the pores are compressed until all larger pores have been compressed. The cumulative pore volume curve of remolded loess of any compaction degree can be divided into two segments, large-pore segment (6–50 μm) and small-pore segment (< 6 μm). The large-pore segment is simplified into a horizontal line and a straight line which slope is independent on the compactness.

Conclusions Remolded loess has very different microstructure and PSD from intact loess even though they may have the same GSD (grain-size distribution), mineralogical composition, and some other physical properties. The microstructural evolution induced by mechanical loading also varies in both kinds of soils. Based upon the measured PSDs, a method is proposed for predicting the PSD of remolded loess of any compaction degree using a reference PSD.

Keywords Consolidation · Intact loess · Microstructural evolution · MIP · PSD · Remolded loess

Responsible editor: Fanghua Hao

✉ Ping Li
lp19881028@163.com

¹ Department of Geology, Northwest University, Xi'an 710069, China

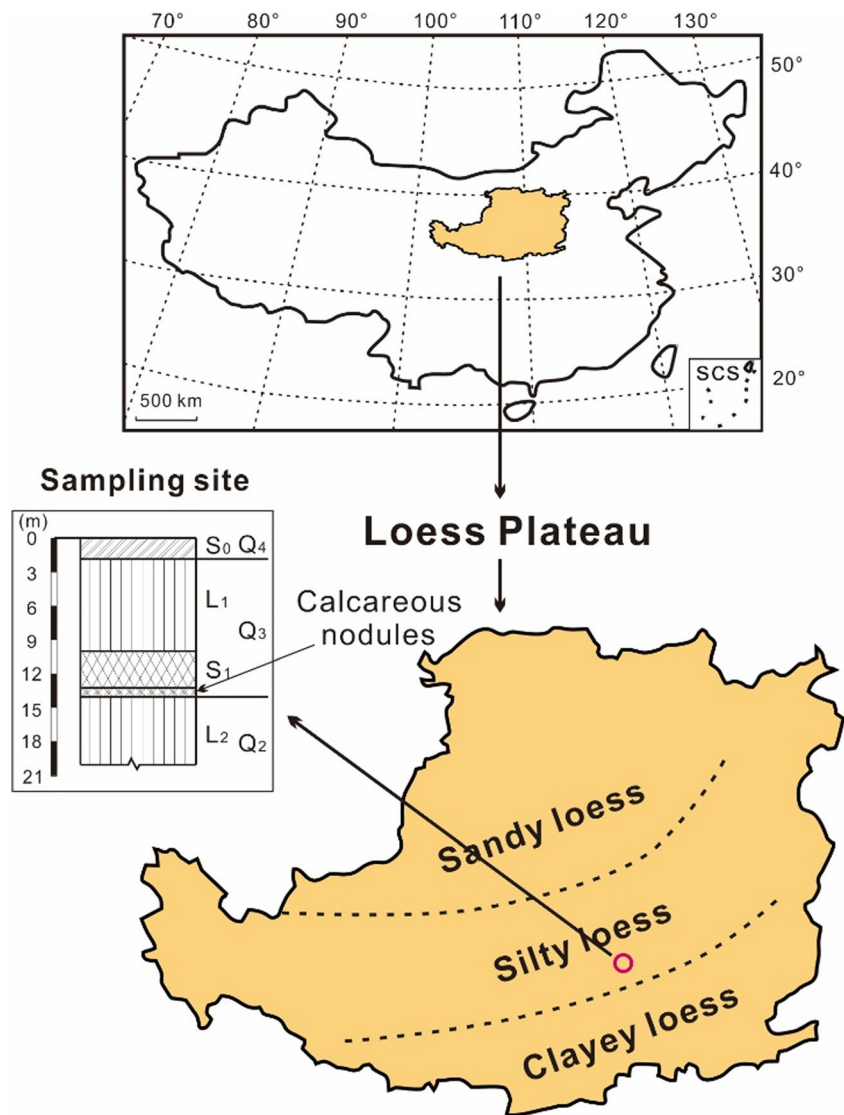
² State Key Laboratory of Continental Dynamics, Northwest University, Xi'an 710069, China

³ Department of Civil Engineering, University of Ottawa, Ottawa, ON K1N6N5, Canada

1 Introduction

Loess soils are widely distributed in semi-arid and arid regions around the world, including countries such as China, Russia, and the USA. In China, loess soils have deposited since 2.4 million years (i.e., 2.4 Ma) ago, generating the well-known Loess Plateau extending an area of over 440,000 km², see Fig. 1 (Yao et al. 2012; Gao and Shao 2012). With the approaching of various national and regional development programs, infrastructure constructions in northwest China have experienced an unprecedented growth. In the construction of

Fig. 1 Sampling site of Luochuan on the Loess Plateau of China



infrastructure facilities, locally available materials are always used as the material of subgrade and subbase to reduce the engineering budget. Loess, behaving well as one of building materials at its natural state, is widely used as subgrade or subbase for such as highway and embankment in loess regions.

Loess soils are typically a kind of clayey silt and have an open structure. Such an open structure is characterized by a random particle arrangement, high porosity, and significant amount of macro pores, all these characteristics could be attributed to silt-dominated grain-size composition and aeolian origin of loess soils. For example, in China, soil materials from Gobi Desert were brought by wind to the Loess Plateau since the basin-shaped geomorphology of the Loess Plateau is favorable for deposition of aeolian materials. Loess soils are generally in a state of unsaturated condition and susceptible to collapse (i.e., sudden decrease in soil volume) upon wetting or loading (Barden et al. 1973). For this reason,

compaction, as an extensively used technique for improving the engineering properties of soils, is resorted to reducing collapsibility and settlement for loess soils in practice (Chen and Sha 2009, 2010; Ma et al. 2017).

The mechanical behavior of soils either in their intact state or remolded state is significantly influenced by the soil microstructure. The microstructure of intact loess is featured by loose particle arrangement and inter-particle cementation. However, remolded loess may have quite different microstructure from that of intact loess since clay and carbonate cementations could be damaged during remolding, also due to different hydration processes experienced by intact and remolded loess, regardless of that they have the same GSD and mineralogical composition. Therefore, remolded loess would behave in a manner distinct from that of intact loess in response to mechanical changes taken place on soil sample (Xu and Coop 2017; Xu et al. 2018). It is the reason many constitutive models proposed based on the experimental data of remolded

soils fail to be used for naturally deposited soils (Burland et al. 1996; Callisto and Calabresi 1998; Nagaraj et al. 2003). The mechanical behavior of intact loess is observed to approach that of remolded loess when the intrinsic microstructure gradually degrades due to loading or wetting (Hu et al. 2000; Yang et al. 2014). The microstructure of intact loess has been sufficiently studied during last several decades, for interpreting the macro-level mechanical behavior (i.e., collapsibility, permeability, compressibility, et al.) and incorporating the microstructural characteristics into predictions of loess soils' mechanical behavior (Delage et al. 2005; Muñoz-Castelblanco et al. 2012; Fang et al. 2013; Chen et al. 2015; Haeri et al. 2016; Fan et al. 2017; Zhang and Wang 2018; Xu et al. 2018). Among the techniques applied for characterizing the microstructure of a soil, the mercury intrusion porosimetry (MIP) is a very useful technique that can provide quantitative information (Jiang et al. 2014; Wen and Yan 2014; Ng et al. 2016). In a way, the scanning electron microscope (SEM) technique could also provide quantitative information by combining image processing programs. However, it is cumbersome and to some extent subjective since the binary technique is always used to distinguish soil pores from particles in a SEM image. In addition, this method can only provide two-dimensional morphology properties of soil pores or particles (Li et al. 2016).

The microstructure of soils can evolve as a result of any mechanical, hydraulic, chemical, or thermal change taken place on soil sample. Quantitative characterization of the microstructural evolution under complicated stress paths of loess soils is crucial for predictions of their mechanical behavior. However, a few investigations have been conducted to reveal the evolution of the microstructure or pore-size distribution (PSD) for loess soils (Jiang et al. 2014). In comparison, many researches were performed on clayey soils. Griffiths and Joshi (1989) investigated the microstructural evolution due to consolidation for four clayey soils by using the MIP technique. They concluded that the increase in consolidation stress results in an increase in pore volumes between 0.1 and 0.8 μm , which is accounted for the reduction of pore spaces greater than about 0.8 μm ; while pore volumes less than 0.1 μm remain constant regardless of consolidation stress. Thom et al. (2006) characterized the microstructures of both compacted and reconstituted kaolin samples that had been saturated and consolidated under different stress levels. The bimodal PSD is observed to be initially destructed as applied stress is increased. While the bimodal nature redevelops under higher stresses, which is attributed to the shrinkage of aggregates generated by unloading under undrained condition. Monroy et al. (2010) stated that the microstructural evolution of a compacted clay (molded at dry of optimum state) due to loading is stress-path-dependent, and that due to wetting is dependent on the stage of hydration. Delage (2010) measured the PSD of a remolded medium sensitivity

clay. Intra-aggregate pores are suggested not to be compressed until all larger pores have collapsed during consolidation (a porosimeter with measurable pore radius of 0.005–5 μm was used, the largest entrance pore radius in the studied clay is approximately 1 μm). Recently, Jiang et al. (2014) investigated the microstructural evolution of an intact loess and its remolded counterpart in triaxial tests along two different stress paths. The results showed that loading leads to a significant compression of inter-aggregate pores, without modifying intra-aggregate pores (i.e., < 0.1 μm) for both kinds of soils. The influence of loading on inter-aggregate pore volumes is stress-path-dependent. Ng et al. (2016) observed a clear shift of macro pores towards smaller-sized pores in an intact loess due to consolidation pressure increase; while inundation and consolidation have unnoticeable effect on micro pores (< 0.2 μm defined in their study). More recently, Shao et al. (2017) tested several remolded loess specimens (molded at dry of optimum state) which initial water contents were modified before consolidation tests. The results indicate that there is no apparent change in the PSD during wetting. The above review suggests that current understanding of the microstructure of loess soils is limited because there is little information about the microstructural evolution of loess soils under complicated stress paths. This could be attributed to the difficulty in accessing to advanced equipment and complexity related to handling these apparatuses.

For this reason, in the present study, the microstructures of intact loess specimens consolidated to various vertical pressures and remolded loess specimens with various compaction degrees are characterized using the SEM and MIP techniques. Remolded soil of a varying compaction degree is equivalent to consolidate the remolded loess with the least compaction degree to a varying stress level". The microstructural evolution due to consolidation is investigated for both intact loess and remolded loess. The results show that the microstructure and evolution of microstructure or PSD of intact loess are very different from that of remolded loess. Based on the test results, a method is proposed for predicting the PSD of remolded loess of any compaction degree using a reference PSD.

2 Material and methods

2.1 Test material

The loess samples were collected from Luochuan, central Loess Plateau of China for conducting investigations in the present study (see Fig. 1). The soil profile of the sampling site consists of loess soils deposited in the Holocene (Q_4) and late and middle Pleistocene (Q_3 and Q_2), respectively. Q_2 loess is further sub-divided into dozens of loess stratums sandwiched by paleosol stratums (see Fig. 1, L represents loess and S represents paleosol). Loess and paleosol are different in terms

of field magnetic susceptibility, which reflects the concentration of ultrafine magnetite, relates to the degree of pedogenesis, and thus serves as a measure of climate (An et al. 1989). In that case, the exposed loess soils belong to S_0 , L_1 , S_1 , and L_2 . In paleosol soils that are relatively impermeable, calcareous nodules are occasionally concentrated. It could be because water infiltration in loess soils results in leaching of Ca^{2+} ions, which accumulate in paleosol soils and react with atmospheric CO_2 (as shown in Fig. 1). The block samples were retrieved by hand at a depth of 4 m in an exploratory well that was excavated at the sampling site. Block samples were then covered and sealed by several layers of plastic film and wax to preserve the soil structure and minimize loss of water content. The samples were put inside wood chip-filled boxes and transported to the laboratory for performing various tests.

The soil studied belongs to L_1 , its physical properties were determined following relevant ASTM standard test methods and are summarized in Table 1. The GSD shows that the test material consists mainly of silt particles (i.e., 0.005–0.075 mm) with a fraction of 75.1%. According to the United Soil Classification System, the soil classifies as a low-plasticity clay (CL). Mineral composition of the test material was characterized by X-ray diffraction (XRD) technique. Results of semi-quantitative XRD analysis determined using the method suggested by Moore and Reynolds (1997) are summarized in Table 2.

2.2 Preparation of specimens

Oedometer specimens were extracted from intact block samples with the aid of greased steel ring of 80 mm in diameter and 20 mm in height. In total, five intact specimens having a weight of 0.146 ± 0.003 kg were used for consolidation tests. Intact loess specimens were incrementally loaded to vertical pressures of 100, 200, 400, 600, and 800 kPa in oedometer cells, respectively. Under each load increment, dial readings were taken every half an hour until less than 0.01 mm compression occurs per hour. This process was repeated until vertical pressure, which was doubled for each load increment, was equal to the desired value. After the test, the specimen was carefully taken out from the apparatus

and stored in a humid environmental chamber for performing SEM and MIP tests.

Disturbed loess soils were pulverized using a rubber mallet, air-dried for several days, and passed through a 0.5-mm sieve. This is done to disintegrate aggregations and break interconnections in intact loess. The soil was then mixed with a predetermined amount of de-aired water to achieve the optimum water content (i.e., 18%, determined using the Proctor compaction test following ASTM D1557). The wet soil was sealed in plastic bag and stored in a humid chamber for a period of at least 48 h to allow an equalization of water content throughout the soil. After that, the wet soil was filled in a mold of 38 mm in diameter and 80 mm in height and statically compressed using a strain-controlled sampling apparatus. Remolded loess soils of six dry densities, i.e., 1.31, 1.40, 1.49, 1.58, 1.67, and 1.75 kg/m^3 , were produced. With respect to the maximum dry density (i.e., 1.75 kg/m^3), the six remolded soils have a compaction degree of 0.75, 0.80, 0.85, 0.90, 0.95, and 1.00, respectively.

To investigate the microstructural evolution in intact and remolded loess due to loading, the microstructures of remolded loess soil of a varying compaction degree and intact loess both before and after consolidation test were characterized using the SEM and MIP tests. In total, SEM and MIP tests were performed on 12 specimens.

2.3 SEM tests

Cubic sticks with the dimensions of 10 mm × 10 mm × 20 mm (length × width × height) were trimmed out from intact block sample, remolded specimens, and oedometer specimens after consolidation tests. The sticks were dehydrated in a freeze dryer using liquid nitrogen at a temperature below -70 °C. In contrast to oven-drying and air-drying, freeze-drying method has the advantage of eliminating surface tension caused by air-water interfaces, and thus the expansion and shrinkage of soil specimen were restricted to a low level, resulting in minimal disturbance to the soil structure (Delage and Lefebvre 1984; Romero and Simms 2008). Before microstructural observation, each soil stick was fractured carefully at approximately 10 mm height. One-half stick was stuck to the shooting

Table 1 Physical properties of the test material

In situ water content w (%)	In situ density ρ (Mg/m ³)	Specific gravity G_s	Atterberg limits (%)			Grain-size distribution (mm, %)			Classification
			Liquid limit w_L	Plastic limit w_P	Plasticity index I_P	Sand (>0.075)	Silt (0.075–0.005)	Clay (<0.005)	
9.9	1.46	2.71	28.2	17.7	10.5	15.1	75.1	9.8	CL
ASTM D2216	ASTM D1557	ASTM D854	ASTM D4318			ASTM D422			ASTM D2487

Table 2 Mineralogical composition of the test material

Mineral	Quartz	Plagioclase feldspar	Potash feldspar	Calcite	Hornblende	Illite	Chlorite
Content (%)	43.6	16.1	4.2	14.6	1.5	10.5	9.5

pad using electron-conductive tape without disturbing the fractured plane. The selected fractured plane was sputter-coated with platinum (i.e., Pt) in an ion sputtering equipment and used for microstructural observation, using a FEI Quanta 400 FEG scanning electron microscope.

2.4 MIP tests

Cubes of 1 cm³ were trimmed out from intact block sample, remolded specimens, and oedometer specimens after consolidation tests. The cubes were dehydrated in the manner as same as that for SEM tests. Autopore IV 9500 mercury intrusion porosimetry with a maximum intrusion pressure of 227.5 MPa was used for characterization of the PSD.

Dry soil cubes were placed inside the porosimetry and a vacuum was firstly applied. A non-wetting fluid, mercury, was then allowed to enter the chamber containing soil cubes, and the pressure in mercury was subsequently increased in steps. This caused mercury to progressively penetrate the voids, from the larger to the smaller. The volume of mercury entering the cube at each pressure increment was continuously monitored; the cumulative volume of mercury that is identical to the cumulative pore volume can be easily obtained. Given the simplified assumption of cylindrical pores and according to the Laplace's capillarity law, a relation between the penetration pressure, P_{Hg} , and corresponding entrance pore diameter, D , can be written as

$$P_{\text{Hg}} = -\frac{4\sigma_{\text{Hg}}\cos\theta}{D} \quad (1)$$

where P_{Hg} is the pressure in the mercury required to penetrate a pore of D in diameter, σ_{Hg} represents the surface tension of mercury, and θ denotes the contact angle between the mercury and the pore walls. In the present study, $\sigma_{\text{Hg}} = 0.485$ N/m and $\theta = 130^\circ$ were adopted (Diamond 1970; Griffiths and Joshi 1989; Delage et al. 1996; Monroy et al. 2010; Jiang et al. 2014).

During the penetration of mercury, the soil cube was initially surrounded with the mercury at a low pressure of 3.6 psi (approximately 25 kPa), which corresponds to a pore diameter of 50 μm . Thus, the MIP technique cannot measure the pores larger than 50 μm . Then, the mercury pressure was increased in steps to 33,000 psi (approximately 228 MPa) which corresponds to a pore diameter of 5.5 nm; thus, the pores smaller than 5.5 nm cannot be detected. In addition, the enclosed pores and constricted pores could not be measured using the MIP technique; these kinds of porosity will be discussed in the

following sections (Griffiths and Joshi 1989; Jiang et al. 2014; Ng et al. 2016). In addition, intact soil structure may be disturbed in early stages of mercury penetration when the pores are mostly empty. Despite these limitations, many researchers have successfully characterized the microstructures of loess soils using the MIP method (Delage et al. 2005; Jiang et al. 2014; Wen and Yan 2014; Ng et al. 2016).

3 Results and discussion

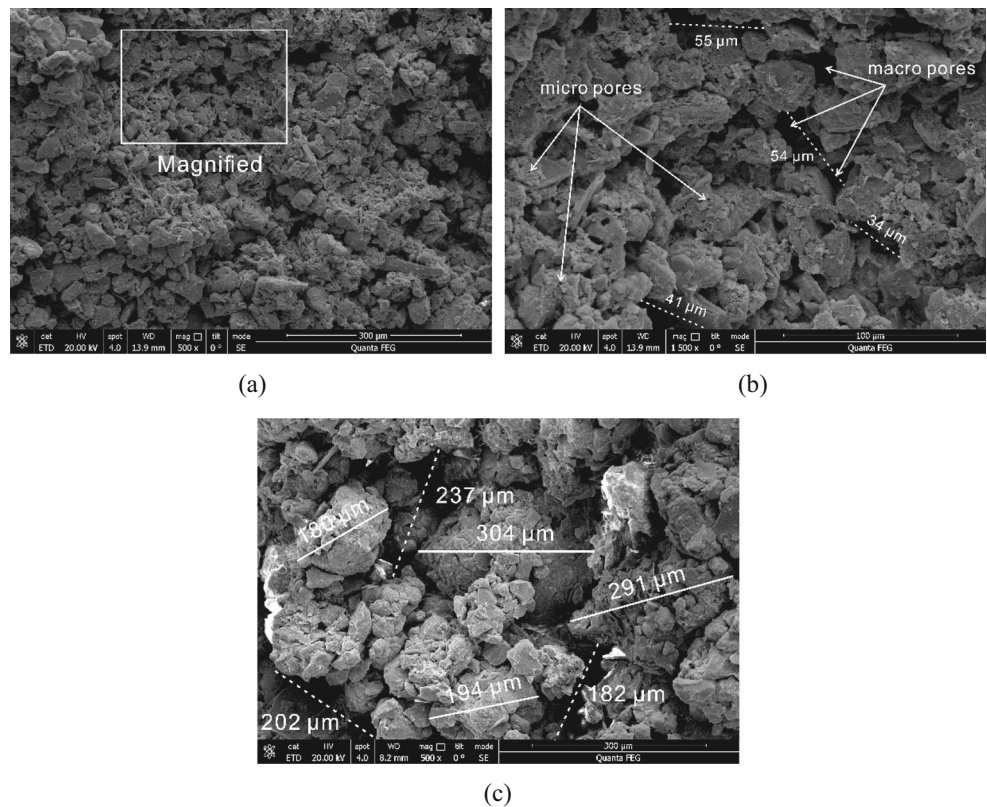
3.1 Microstructures of intact and remolded loess

The microstructure of intact loess is introduced and compared with that of the same soil in remolded state in this section, for better interpretation of the microstructural evolution due to mechanical changes in both soils. The focus is directed to four elements commonly used to characterize the microstructure of a soil, namely, particles, pores, contacts, and cementations (Li et al. 2016).

Figure 2 depicts the micrographs of intact loess and remolded loess with a compaction degree of 0.75. From Fig. 2a which is magnified in Fig. 2b, it can be seen that silt particles (attached with small-sized clay aggregates) and (sand-) silt-clay aggregates dominate in the intact loess soil structure. In intact loess, aggregates are developed mainly due to reprecipitation of clay and carbonate cementations on the particle surfaces and at the particle contacts, cementing elementary particles (i.e., clays, silts, and sands) together. Owing to the angularity of silt particles, varying morphology of cementations, and existence of matric suction, silt particles and aggregates are randomly orientated and loosely arranged. This renders the soil an open and potentially metastable structure. The pores can be divided into two sets in accordance with the particle arrangement. The pores inside clay aggregates are defined as intra-aggregate pores or micro pores, while the pores among aggregates or coarse particles are termed inter-aggregate (and inter-particle) pores or macro pores (i.e., > 0.1 μm , refer to Collins and McGown 1974). Inter-aggregate pores make up the majority of the pore volume, and most inter-aggregate pores are connected to each other through narrow channels. In other words, intact loess soil has a two-level structure (i.e., macro-level structure and micro level structure) along with a dual PSD.

In loess soils, clay and carbonate cementations play the most important role in cementing particles and supporting the soil structure, in comparison to soluble bonding agents,

Fig. 2 Micrographs of **a** intact loess at overall view, **b** intact loess at local view, and **c** remolded loess with a compaction degree of 0.75



matric suction, and other attractions (Gao 1981; Derbyshire and Mellors 1988; Rogers et al. 1994; Jiang et al. 2014). Clay cementations are clearly observable. In the micrographs, clays are seen to coat coarse particles (in the form of small-sized aggregate), to aggregate silts into silt-clay aggregates and to connect particles (in forms of bridge and buttress), instead of functioning individually. However, direct observation of carbonate cementations is difficult due to their special morphology as coatings or bridges (Liu et al. 2016). The presence of carbonate cementations however can be identified by mineralogical characterization, and from mechanisms for possible formation of carbonate cementations, either. The loess soil studied contains considerable amount of calcite (i.e., CaCO_3), 14.6% (see Table 2). Calcite can be both primary and secondary; primary calcite is inherited from initial wind-blown deposits and usually presents as solid particles. Weathering of primary calcite can result in leaching of Ca^{2+} which can then react with atmospheric CO_2 (i.e., $\text{CaCO}_3 + \text{CO}_2 + \text{H}_2\text{O} \rightarrow \text{Ca}(\text{HCO}_3)_2$), while re-dehydration can lead to reprecipitation of CaCO_3 (secondary calcite or carbonate cementations) (i.e., $\text{Ca}(\text{HCO}_3)_2 \rightarrow \text{CaCO}_3 + \text{CO}_2 + \text{H}_2\text{O}$) (Derbyshire 2001; Delage et al. 2005). Therefore, both clay and carbonate cementations are coating coarse particles, bridging and buttressing coarse particles and silt-clay aggregates in loess soils.

The remolded loess soil with a compaction degree of 0.75 has similar void ratio with intact loess (i.e., 1.05 and 1.04,

respectively), while the microstructure of remolded loess, as shown in Fig. 2c, is very different from that of intact loess (Fig. 2a). In general, intact loess has a more homogeneous structure than remolded loess. Aggregates (with much greater size than that in intact loess) are fundamental elements in remolded loess, and few clean sand or silt particles can be seen. In remolded loess, electronegativity of clay platelets, high van der Waals attraction, and matric suction between

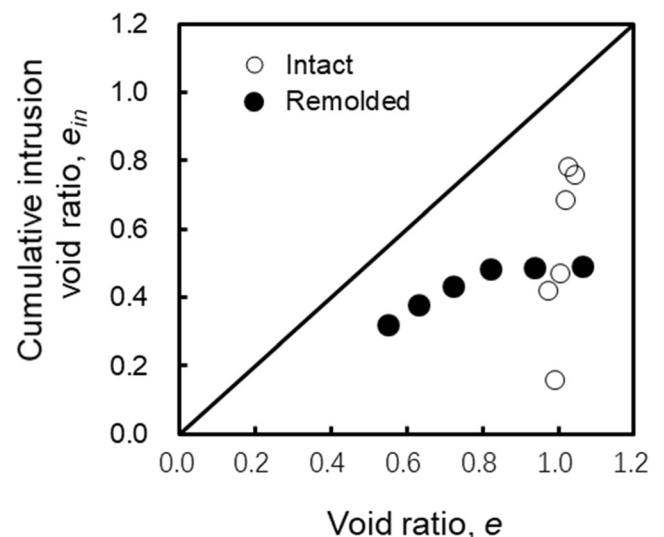
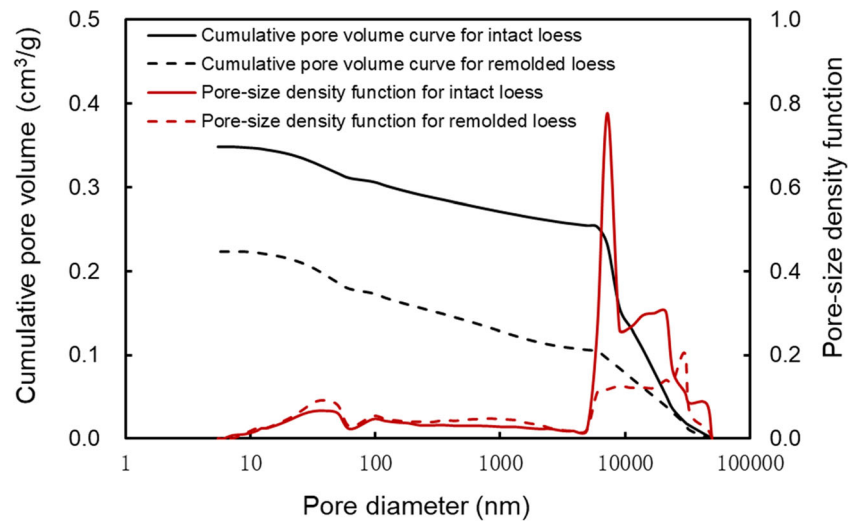


Fig. 3 Comparison between void ratio and cumulative intrusion void ratio

Fig. 4 PSDs of intact loess and remolded loess with the same void ratio



particles mainly contribute to the development of aggregates. In particular, on dry side of the optimum state, there would not be sufficient water to allow a complete development of double layer of ions electrically attracted to clay platelets, such that the distance between two clay platelets would be small

enough for attractions (van der Waals attraction and matric suction) to be dominated (Delage et al. 1996). Under such conditions, more aggregates and aggregates with greater size could be developed. In Fig. 2c, aggregates with the size up to 300 μm make up the soil skeletal structure, imparting

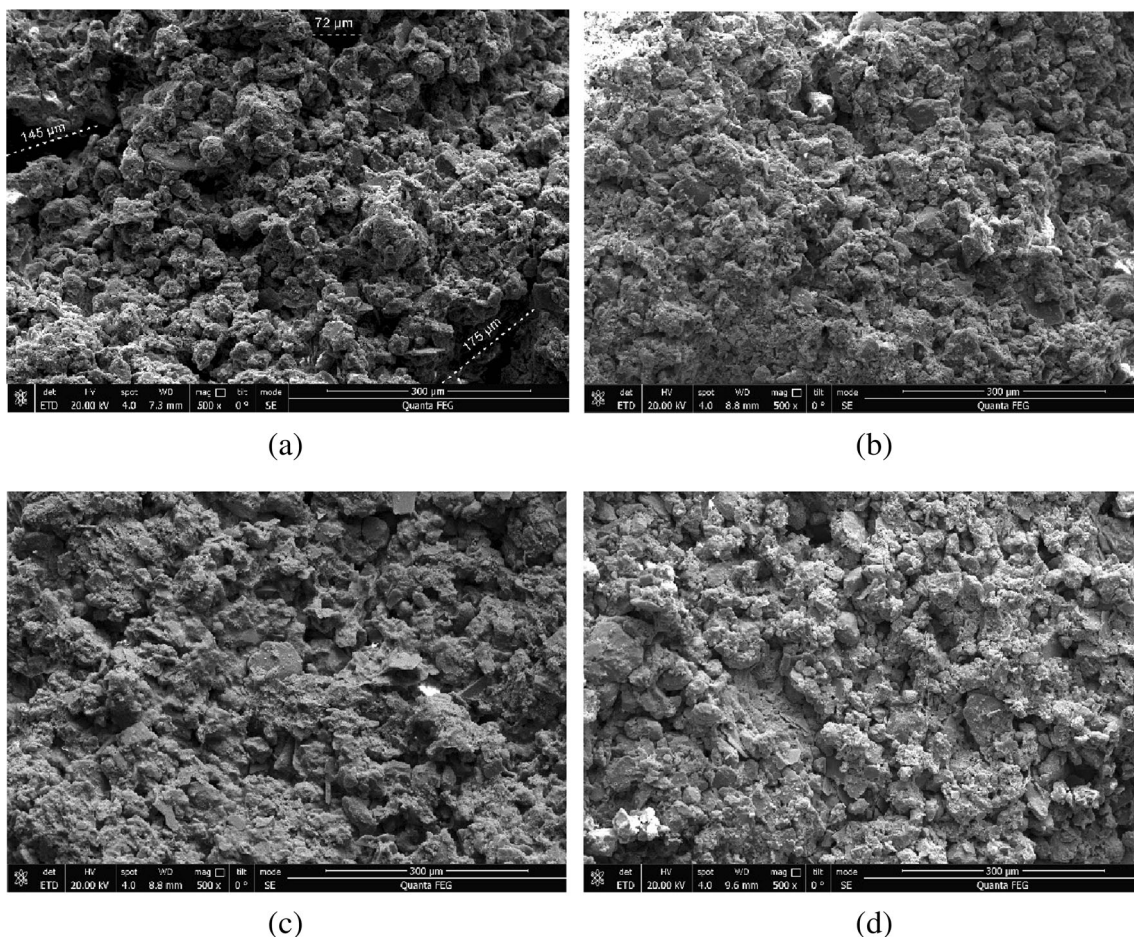


Fig. 5 Micrographs of intact loess specimens consolidated to various vertical stresses. **a** 200 kPa. **b** 400 kPa. **c** 600 kPa. **d** 800 kPa

remolded loess a distinct two-level structure. Some inter-aggregate pores, which entrance diameter could be too large to be detected using the MIP technique (i.e., $> 50 \mu\text{m}$), are observed in Fig. 2c.

3.2 Pore-size distribution

With the MIP technique, the PSD of a soil can be presented in terms of either cumulative pore volume or pore-size density function. The pore-size density corresponds to the derivative of the cumulative pore volume with respect to the logarithmic entrance pore diameter, i.e., $\partial v/\partial \log D$. The cumulative intrusion void ratio, e_{in} , is obtained by dividing the cumulative volume of the intruded mercury by the volume of soil cube. Figure 3 compares the cumulative intrusion void ratio, e_{in} , with the void ratio, e , obtained from mass-volume relations of all specimens (including intact loess specimens consolidated to various vertical pressures and remolded loess specimens of various compaction degrees). In general, e_{in} is smaller than e , which can be attributed to several reasons (or limitations of the MIP technique): (i) pores that are isolated by surrounding solid particles will not be measured (enclosed porosity); (ii) pores that are accessible only through smaller channels will not be detected until the smaller channels are penetrated (constricted porosity); (iii) pores that are too large to be detected with the minimal pressure the equipment is able to deliver (non-detected porosity); and (iv) pores that are too small to be intruded with the maximum practical pressure of the available equipment (non-intruded porosity) (Delage and Lefebvre 1984; Romero and Simms 2008; Ng et al. 2016). Among these four kinds of pores, the discordance arisen between e_{in} and e for intact loess is probably partly due to the constricted porosity since a dramatic decrease of e_{in} takes place even though e decreases slightly. That means the constricted porosity is strengthened due to the increasing consolidation pressure. In a study by Ng et al. (2016), constricted pores were observed to occupy a significant fraction in the structure of a loess from Xi'an, China. This discordance is also attributed to the non-detected porosity and non-intruded porosity (see Fig. 2b). In addition, sample variability may make a contribution to this discordance for intact loess. However, the discordance for remolded loess could be mainly due to non-detected pores with the entrance diameter greater than $50 \mu\text{m}$ since e_{in} is approaching e as the compactness is increased. That means the non-detected porosity is weakened with the increasing compactness (or compaction energy). In Fig. 3, in general, the variation of e_{in} is consistent with that of e , especially for remolded loess. Therefore, the MIP technique could be used to reasonably characterize the PSD in a loess soil over a wide range of pore size.

Figure 4 shows the PSDs of intact and remolded loess soils in terms of both cumulative pore volume and pore-size density function in semi-logarithmic plots. The bimodal characteristic

of the PSD mentioned earlier is evidenced here by two peaks on the density curves, defining two major pore series in the soil structure. The first pore series of inter-aggregate type with a dominant macro-pore diameter is about $7 \mu\text{m}$ for intact loess and about $30 \mu\text{m}$ for remolded loess. A second pore series of intra-aggregate type has an identical dominant micro pore diameter of about $0.04 \mu\text{m}$ for both soils. A great difference is observed between the cumulative volumes of mercury intruded into intact and remolded loess cubic samples although both soils have the same void ratio. This difference is mainly due to the non-detected porosity with the entrance diameter larger than $50 \mu\text{m}$ in remolded loess, as discussed earlier. In general, the cumulative and density curves of two soils presented in Fig. 4 are close to each other for the entrance diameter up to $6 \mu\text{m}$, indicating that the mode of formation (natural deposition or compaction) has little influence on the pore series with small dimension (i.e., $< 6 \mu\text{m}$). In comparison, remolded loess has a little higher density of intra-aggregate pores as well as the pore series with medium dimension (i.e., between 0.1 and $6 \mu\text{m}$). Intact loess has a higher density in the pore series between 6 and $25 \mu\text{m}$, which would include a number of

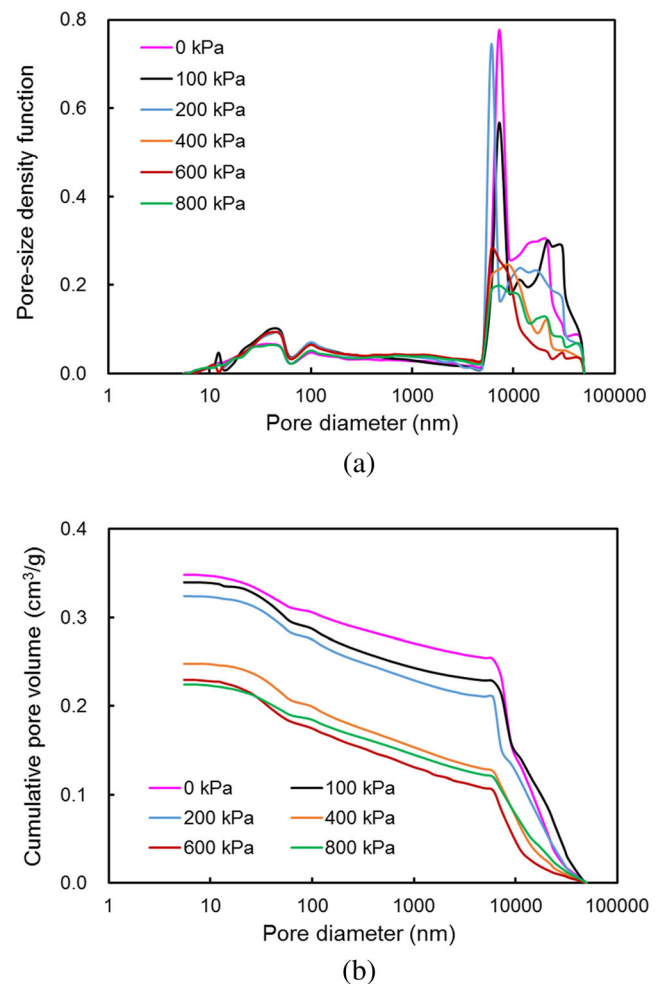


Fig. 6 PSDs of intact loess specimens consolidated to various vertical pressures. **a** Pore-size density function. **b** Cumulative pore volume curve

constricted pores. In short, the PSDs of intact loess and remolded loess are quite different even though they have the same void ratio; as a result, they can behave differently in response to mechanical and hydraulic changes.

3.3 Influence of consolidation on the intact loess microstructure

Figure 5 summarizes the micrographs of intact loess specimens that were consolidated in oedometer cells to various vertical pressures. The axial displacements were measured as 0.161, 0.254, 0.384, 0.525, and 0.681 mm, corresponding to the axial strains of 0.81%, 1.27%, 1.92%, 2.63%, and 3.41% under the vertical pressures of 100, 200, 400, 600, and 800 kPa, respectively. In agreement with the results of oedometer tests, it can be seen from the SEM images that the increasing consolidation pressure has inconspicuous influence on the intact soil microstructure. However, a close comparison between the micrograph of specimen consolidated to 200 kPa (as shown in Fig. 5a) and the micrographs of specimens to higher vertical pressures (i.e., 600 and 800 kPa, Fig. 5b–d) suggests that the higher the vertical pressure, the less the

inter-aggregate pore volumes; the soil structure is closer and more homogeneous as the consolidation pressure is increased.

Figure 6 shows the PSDs of intact loess specimens after consolidation tests. In general, a distinct reduction in inter-aggregate pore series is induced by a vertical stress increase, resulting in a distinct reduction in the cumulative volume of intruded mercury. The bimodal nature of the PSD is not eliminated by consolidation under the stress levels adopted in the present study (i.e., ≤ 800 kPa) while it is diminished with the increasing consolidation pressure. The cumulative and density curves under various vertical pressures are similar in shape for the entrance diameter up to $6 \mu\text{m}$, suggesting that the pores with the entrance diameter smaller than $6 \mu\text{m}$ are almost not influenced by consolidation. It is interesting to note that a great decrease in the pores with the entrance diameter larger than $6 \mu\text{m}$ takes place in response to a vertical stress increase from 200 to 400 kPa. It is validated by the significant decrease in the cumulative volume of intruded mercury, from 200 to 400 kPa (see Fig. 6b). This stress level does correspond to the curvature on the compression curve of intact loess, which is termed structural stress of intact loess (Shao et al. 2004). The compression curve of intact loess can generally approximate

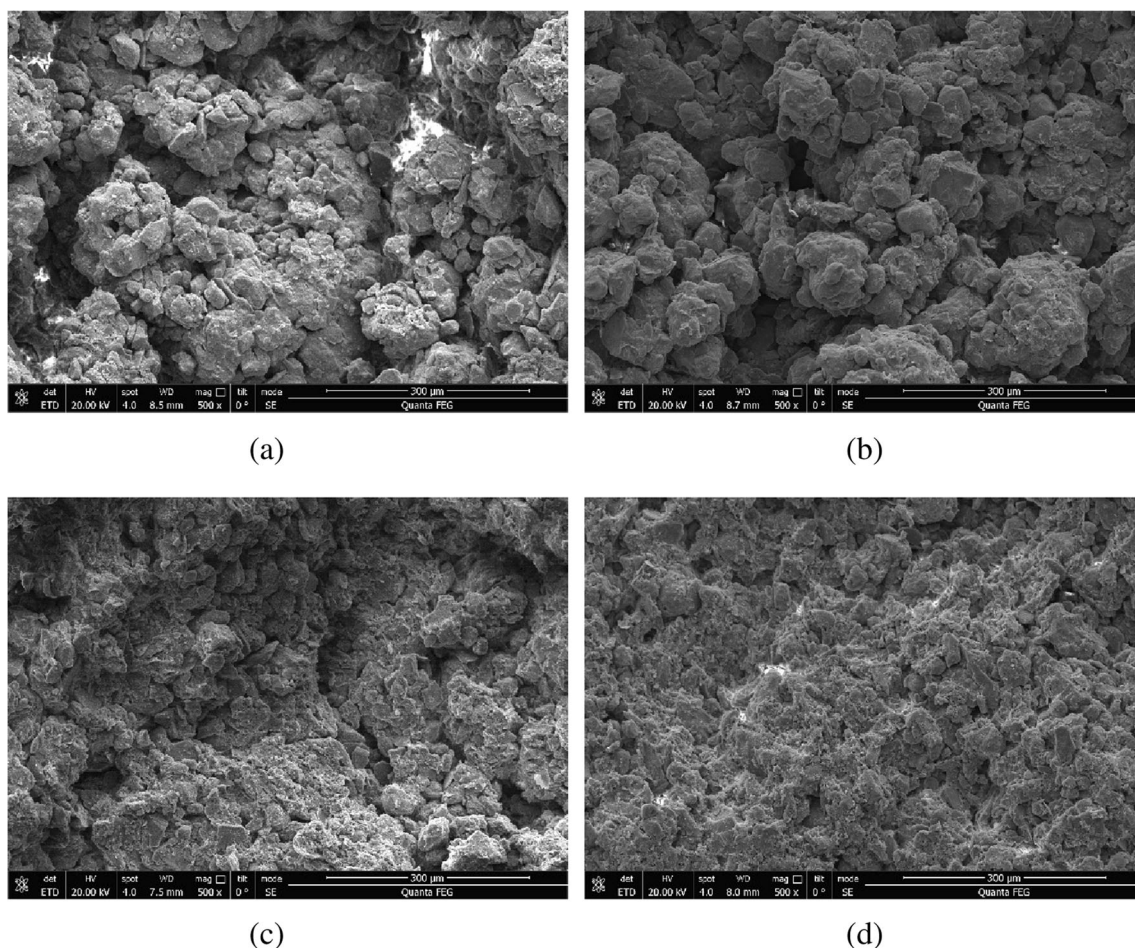


Fig. 7 Micrographs of remolded loess specimens with various compaction degrees. **a** 0.80. **b** 0.85. **c** 0.95. **d** 1.00

into two lines of near-constant slope, the stress level at the curvature is referred to as structural strength of intact loess, which includes the contribution clay and carbonate cementations mainly make to compressive strength. When the soil is subjected to a stress lower than structural stress, small volumetric deformations take place and the soil structure remains intact. However, the soil undergoes significant volumetric compression in response to load increase and the soil structure alters due to bonding breakage as applied stress increases beyond structural strength (Hu et al. 2000).

3.4 Influence of consolidation on the remolded loess microstructure

Figure 7 summarizes the micrographs of remolded loess specimens of various compaction degrees, which were molded using static compaction method with an increasing compaction energy. It is equivalent to consolidate the remolded loess

which has the least compaction degree (i.e., 0.75) under various stress levels. In comparison to intact loess, the increasing consolidation pressure (i.e., compactness) has a significant influence on the remolded soil structure. The soil fabric is observed to transform from an aggregate type into a matrix type in response to increase in consolidation pressure (or compaction energy). Consolidating remolded loess leads to a closer arrangement of aggregates. In addition, the aggregate morphology is also modified by loading to achieve a closer arrangement of aggregates (see Fig. 7c, d).

Figure 8 shows the PSDs of remolded loess specimens with three different compaction degrees. It is shown that, like intact loess, the pores with the entrance diameter less than 6 μm are almost not affected by consolidation since the cumulative and density curves are similar in shape for the entrance diameter up to 6 μm, irrespective of the compactness (see Fig. 8b, the dashed curves are obtained by shifting the curve of remolded loess with a compaction degree of 0.75 downwards). In response to an

Fig. 8 PSDs of remolded specimens with various compaction degrees. **a** Pore-size density function. **b** Cumulative pore volume curve

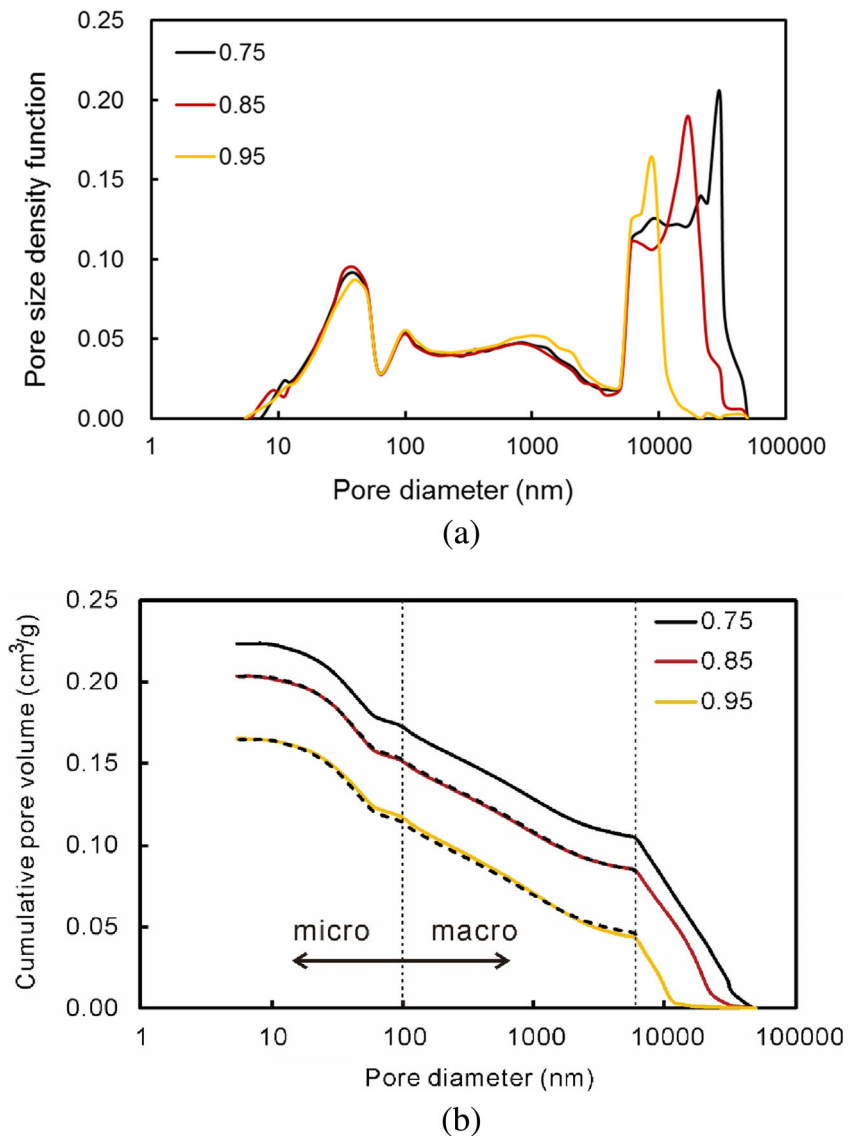
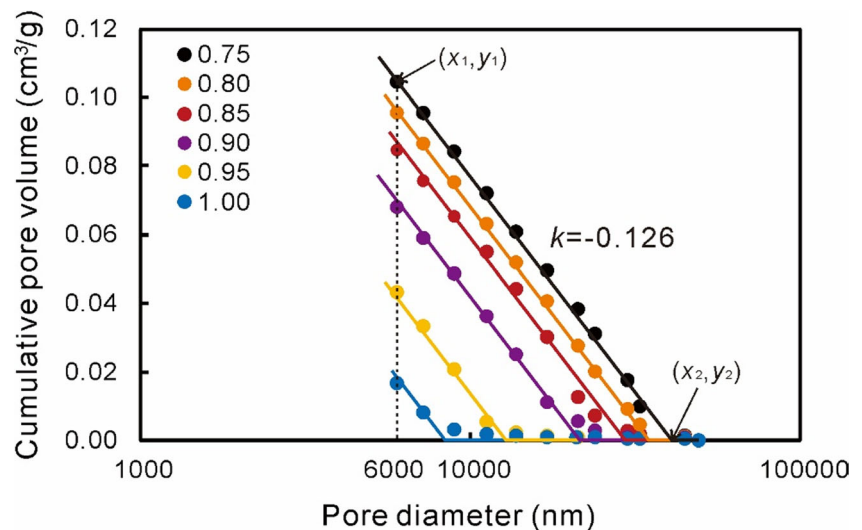


Fig. 9 Large-pore segments of the cumulative curves of the remolded loess soils with various compaction degrees



increase in consolidation pressure, not only does the density of inter-aggregate pores with entrance diameter larger than $6\ \mu\text{m}$ decrease but also the peak that defines the dominant macro-pore diameter on the density curve moves leftward. It is therefore suggested that, unlike intact loess in which inter-aggregate pores with entrance diameter larger than $6\ \mu\text{m}$ are compressed randomly due to loading, the pores in remolded loess are compressed until all larger pores have been compressed. It could be because clay and carbonate cementations at the particle contacts in intact loess contribute to preventing inter-aggregate pores nearby from being damaged; the more cementations at the particle contacts surrounding an inter-aggregate pore, the more difficult for the pore to be compressed. In other words, the structural stability is influenced by both the pore size and the number of cementations at the particle contacts surrounding inter-aggregate pores. While in remolded loess, matric suction contributes much to maintaining the structure stability.

As per the above discussion, the cumulative pore volume curve of remolded loess with any compaction degree can be divided into two segments, one is for the pores with entrance diameter between 6 and $50\ \mu\text{m}$ (i.e., large-pore segment) and the other is for the pores with entrance diameter less than $6\ \mu\text{m}$ (i.e., small-pore segment). The large-pore segment can be simplified into a horizontal line representing zero cumulative pore volume and a straight line which slope is constant (i.e., $k = -0.126$) and independent on the compactness (see Fig. 9). The straight line can be determined by two data points, (x_1, y_1) and (x_2, y_2) ; where x represents entrance diameter and y represents cumulative volume of the pores with entrance diameter greater than x : $x_1 = 6\ \mu\text{m}$ and $y_2 = 0\ \text{cm}^3/\text{g}$; x_2 is the intercept of the straight line on horizontal axis, and it is in actual the maximum entrance diameter measured by mercury intrusion method in the soil and is decreasing with the increasing consolidation pressure. The value of x_2 reduces at a decreasing rate with compaction degree. The relationship between x_2 and compaction degree, C , could be described using a logarithmic

function, as shown in Eq. (2) and Fig. 10. The small-pore segment of the cumulative curve is parallel to that of a specimen with smaller compaction degree, and this segment can be obtained by shifting the curve for a smaller compaction degree downwards by y_1 (see Eq. (3)); y_1 is equal to the cumulative pore volume reduction induced by consolidation. Under such a scenario, the PSD of remolded loess of any compaction degree could be predicted using a reference PSD. For example, with the values of x_2 (determined following Eq. (2)) and k (i.e., -0.126), as well as the cumulative curve for the compaction degree of 0.75 are known, the large-pore segment of the cumulative curve for the compaction degree of 0.80, 0.90, or 1.00 is predicted, as shown in Fig. 9. In addition, the cumulative pore volume curves for the compaction degree of 0.80, 0.90, and 1.00 are predicted. A good agreement can be seen between predicted and measured cumulative curves, see Fig. 11. Therefore, the method proposed in the present study can be used to reliably predict the PSD of remolded loess of any compaction degree using a reference PSD; the value of

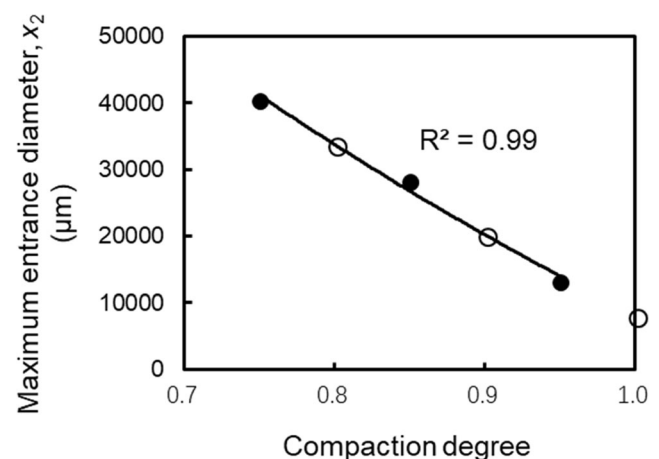
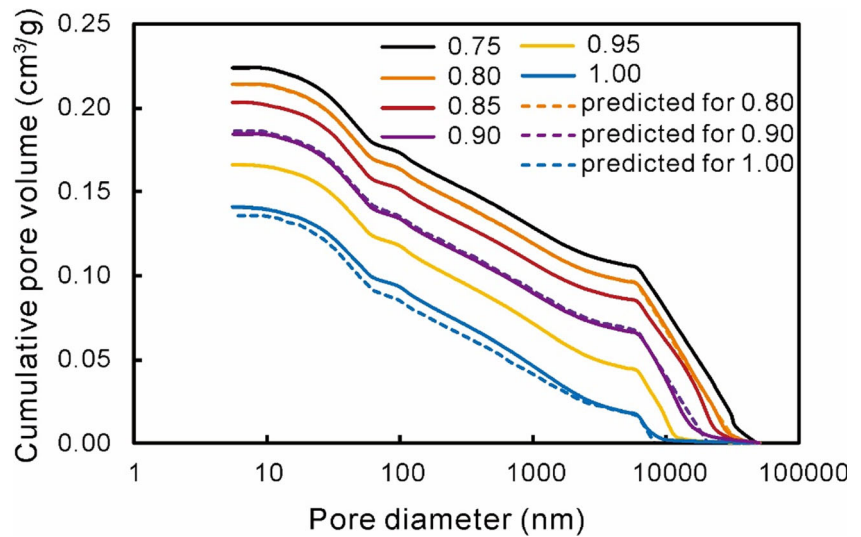


Fig. 10 Relationship between the maximum entrance diameter and compaction degree

Fig. 11 Comparison between predicted and measured PSDs for remolded loess soils with various compaction degrees



parameter k (i.e., -0.126 for the remolded loess tested in the present study) can be determined from the reference PSD. However, the logarithmic relationship between x_2 and C (see Eq. (2) and Fig. 10) needs to be validated for extending this method to other remolded soils.

$$x_2 = -1.15 \times 10^5 \log C + 8.10 \times 10^3 \quad (2)$$

$$y_1 = y_2 + k[\log(x_1) - \log(x_2)] = -0.126 \times [\log(6000) - \log(x_2)] \quad (3)$$

4 Conclusions

Several important conclusions can be reached upon the microstructural characterization of intact loess specimens consolidated to various vertical pressures and remolded loess specimens of various compaction degrees:

- Intact loess has a two-level structure along with a bimodal PSD. The bimodal nature of PSD is not eliminated by consolidation, while it is diminished with the increasing consolidation pressure. The pores with entrance diameter smaller than $6 \mu\text{m}$ are almost not affected by consolidation. However, inter-aggregate pores with entrance diameter greater than $6 \mu\text{m}$ are compressed randomly due to consolidation. It could be because clay and carbonate cementations at the particle contacts contribute to preventing inter-aggregate pores nearby from being damaged. In other words, the structural stability is influenced by both the pore size and the number of cementations at the particle contacts surrounding inter-aggregate pores.
- Remolded loess molded at the optimum state has a distinct two-level structure. However, remolded loess has very

different microstructure and PSD from intact loess even though they may have the same void ratio. Like intact loess, the pores with entrance diameter less than $6 \mu\text{m}$ in remolded loess are almost not influenced by consolidation (or compaction energy), while the pores with entrance diameter greater than $6 \mu\text{m}$ are compressed until all larger pores have been compressed.

- A method is proposed for predicting the PSD of remolded loess of any compaction degree, based upon the microstructural evolution of remolded loess due to consolidation. The cumulative pore volume curve of remolded loess of any compaction degree can be divided into two segments, large-pore segment and small-pore segment. The large-pore segment is simplified into a horizontal line representing zero cumulative pore volume and a straight line which slope is independent on the compactness. The small-pore segment can be obtained by shifting the curve for a smaller compaction degree downwards. The method is used to predict the PSDs of remolded loess soils with different compaction degrees, a good agreement is observed between predicted and measured cumulative curves.

Funding information The authors acknowledge the funding received from the National Natural Science Foundation of China (Grant No. 41630639, 41372269).

References

An ZS, Kukla G, Liu DS (1989) Loess stratigraphy in Luochuan of China. *Quaternary Sci* 9(2):155–168 (in Chinese)

Barden L, McGown A, Collins K (1973) The collapse mechanism in partly saturated soil. *Eng Geol* 7(1):49–60

Burland JB, Rampello S, Georgiannou VN, Calabresi G (1996) A laboratory study of the strength of four stiff clays. *Géotechnique* 46(3): 491–514

Callisto L, Calabresi G (1998) Mechanical behaviour of a natural soft clay. *Géotechnique* 48(4):495–513

- Chen KS, Sha AM (2009) Study of influencing factors of loess compaction. *J Highway Trans Res Development* 26(7):54–58
- Chen KS, Sha AM (2010) Study of deformation characteristics of compacted loess. *Rock Soil Mechanics* 31(4):1023–1029
- Chen Y, Li XA, Huang RQ, Huang L, Li LC, Hong B, Liu ZS, Cai WB (2015) Micro experimental research on influence factors of loess collapsibility. *J Eng Geol* 23(4):646–653 **(in Chinese)**
- Collins K, McGown A (1974) The form and function of microfabric features in a variety of natural soils. *Géotechnique* 24(2):223–254
- Delage P, Lefebvre G (1984) Study of the structure of a sensitive Champlain clay and of its evolution. *Can Geotech J* 21(1):21–35
- Delage P, Audiguier M, Cui YJ, Howat MD (1996) Microstructure of a compacted silt. *Can Geotech J* 33(1):150–158
- Delage P, Cui YJ, Antoine P (2005) Geotechnical problems related with loess deposits in Northern France. *Proceedings of International Conference on Problematic Soils, Famagusta, N. Cyprus*
- Delage P (2010) A microstructure approach to the sensitivity and compressibility of some Eastern Canada sensitive clays. *Géotechnique* 60(5):353–368
- Derbyshire E, Mellors TW (1988) Geological and geotechnical characteristics of some loess and loessic soils from China and Britain: a comparison. *Eng Geol* 25(2):135–175
- Derbyshire E (2001) Geological hazards in loess terrain, with particular reference to the loess regions of China. *Earth-Sci Rev* 54(1):231–260
- Diamond S (1970) Pore size distribution in clays. *Clay Clay Miner* 18:7–23
- Fan XM, Xu Q, Scaringi G, Li S, Peng DL (2017) A chemo-mechanical insight into the failure mechanism of frequently occurred landslides in the Loess Plateau, Gansu Province, China. *Eng Geol* 228:337–345
- Fang XW, Shen CN, Wang L, Chen ZH, Cheng PJ (2013) Research on microstructure of Q₂ loess before and after wetting. *Rock Soil Mech* 34(5):1319–1324 **(in Chinese)**
- Gao GR (1981) Classification of microstructures of loess in China and their collapsibility. *Sci Sinica* 24(7):962–974
- Gao L, Shao M (2012) The interpolation accuracy for seven soil properties at various sampling scales on the Loess Plateau, China. *J Soils Sediments* 12(2):128–142
- Griffiths FJ, Joshi RC (1989) Change in pore size distribution due to consolidation of clays. *Géotechnique* 39(1):159–167
- Haeri SM, Khosravi A, Garakani AA, Garakani AA (2016) Effect of soil structure and disturbance on hydromechanical behavior of collapsible loessial soils. *Int J Geomechanics* 17:04016021. [https://doi.org/10.1061/\(ASCE\)GM.1943-5622.0000656](https://doi.org/10.1061/(ASCE)GM.1943-5622.0000656)
- Hu ZQ, Shen ZJ, Xie DY (2000) Research on structural behavior of unsaturated loess. *Chin J Rock Mech Eng* 19(6):775–779 **(in Chinese)**
- Jiang MJ, Zhang FG, Hu HJ, Cui YJ, Peng JB (2014) Structural characterization of natural loess and remoulded loess under triaxial tests. *Eng Geol* 181:249–260
- Li P, Vanapalli SK, Li TL (2016) Review of collapse triggering mechanism of collapsible soils due to wetting. *J Rock Mech Geotech Eng* 8:256–274
- Liu Z, Liu F, Ma F, Wang M, Bai X, Zheng Y, Yin H, Zhang G (2016) Collapsibility, composition, and microstructure of loess in China. *Can Geotech J* 53(4):673–686
- Ma F, Yang J, Bai X (2017) Water sensitivity and microstructure of compacted loess. *Transportation Geotechnics* 11:41–56
- Monroy R, Zdravkovic L, Ridley A (2010) Microstructural evolution in compacted London Clay during wetting and loading. *Géotechnique* 60(2):105–119
- Moore DM, Reynolds RCJ (1997) X-ray diffraction and the identification and analysis of clay minerals. 2nd edition. Oxford University Press, Oxford
- Muñoz-Castelblanco JA, Pereira JM, Delage P, Cui YJ (2012) The water retention properties of a natural unsaturated loess from Northern France. *Géotechnique* 62(2):95–106
- Nagaraj TS, Miura N, Chung SG, Prasad KN (2003) Analysis and assessment of sampling disturbance of soft sensitive clays. *Géotechnique* 53(7):679–683
- Ng CWW, Sadeghi H, Hossen SB, Chiu CF, Alonso EE, Baghbanrezvan S (2016) Water retention and volumetric characteristics of intact and re-compacted loess. *Can Geotech J* 53:1258–1269
- Rogers CDF, Dijkstra TA, Smalley IJ (1994) Hydroconsolidation and subsidence of loess: studies from China, Russia, North America and Europe. *Eng Geol* 37:83–113
- Romero E, Simms PH (2008) Microstructure investigation in unsaturated soils: a review with special attention to contribution of mercury intrusion porosimetry and environmental scanning electron microscopy. *J Geotech Geol Eng* 26(6):705–727
- Shao SJ, Zhou FF, Long JY (2004) Structural properties of loess and its quantitative parameter. *Chinese J Geotechnical Engineering* 26(4):531–536 **(in Chinese)**
- Shao XX, Zhang HY, Tan Y (2017) Collapse behavior and microstructural alteration of remolded loess under graded wetting tests. *Eng Geol* 233:11–22
- Thom R, Sivakumar R, Sivakumar V (2006) Effects of pressure on the distribution of bi-modal pore size distribution in unsaturated kaolin. *Proceedings of 4th International Conference on Unsaturated Soils, Carefree, United States*
- Wen BP, Yan YJ (2014) Influence of structure on shear characteristics of the unsaturated loess in Lanzhou, China. *Eng Geol* 168(1):46–58
- Xu L, Coop M, Zhang M, Wang G (2018) The mechanics of a saturated silty loess and implications for landslides. *Eng Geol* 236:29–42
- Xu L, Coop MR (2017) The mechanics of a saturated silty loess with a transitional mode. *Geotechnique* 67(7):1–16
- Yang C, Carterjohn P, Sheng DC (2014) Description of compression behaviour of structured soils and its application. *Can Geotech J* 51(8):921–933
- Yao X, Fu B, Lü Y, Chang R, Wang S, Wang Y, Su CH (2012) The multi-scale spatial variance of soil moisture in the semi-arid Loess Plateau of China. *J Soils Sediments* 12(5):694–703
- Zhang F, Wang G (2018) Effect of irrigation-induced densification on the post-failure behavior of loess flowslides occurring on the heifangtai area, Gansu, China. *Eng Geol* 236:111–118